On time delay velocity feedback control of the composite cantilever beam model subjected to multi-excitation forces

Y.A. Amer
Department of Mathematics
Faculty of Science
Zagazig University
Zagazig
Egypt
yaser31270@yahoo.com

Taher A. Bahnasy*
Department of Physics and Engineering Mathematics
Faculty of Engineering
Tanta University
Tanta
Egypt
taher.bahnasy@gmail.com
taher.bahnasy@f-eng.tanta.edu.eg

Ashraf M. Elmhlawy
Department of Physics and Engineering Mathematics
Faculty of Engineering
Tanta University
Tanta
Egypt
A.Almahalawy@f-eng.tanta.edu.eg

Abstract. The vibration rate of a structural dynamic design modelling a nonlinear composite cantilever beam at simultaneous sub-harmonic and internal resonance excitation is suppressed using delayed velocity feedback control (DVFC) in this article. This system of second order differential equations with nonlinearity due to quadratic and cubic terms, excited by parametric and external excitations, is presented. The procedure of multiple time scales perturbation is used to achieve an estimated solution for this scheme. At this approximation order, all potential resonance cases are extracted and numerically investigated. Both frequency response formulas and phase-plane trajectories are used to assess the system's stability during the worst resonance. The outcomes of various parameters on the device and controller are numerically investigated. The simulation results are achieved using Matlab and Maple programs. The time-dependent displacements are provided, and excellent consensus is reached as compared to results produced utilizing the Rung-Kutta procedure.

Keywords: Composite cantilever beam, time delay, multiple time scales method, sub-harmonic resonance, delayed feedback controller, stability analysis.

∗. Corresponding author

1. Introduction

In recent times, composite beams have seen a lot of progress in mechanical science and aerospace. Conscious or smart systems are generated when active devices such as actuators and sensors are incorporated into the composite together with an appropriate control algorithm. They are used to optimize operating parameters or lower structure disruption and vibration. The coupled nonlinear vibration of several mechanical vibration systems can be simplified to nonlinear second order differential equations that can be solved analytically and numerically. The effect of modal correlations on the nonlinear behavior of harmonically disturbed structural and dynamical models was studied theoretically and experimentally by A. H. Nayfeh and B. Balachandran [1] and A. H. Nayfeh et al. [2]. They made discussions about rings, shells, pendulums, arches, ships, beam systems, and surface waves, as well as the parallels in their qualitative behavior. Quadratic nonlinear effects distinguish the structures, which can lead to 2:1 internal and combined parametric resonances. This resonances induce nonlinear periodic, quasi-periodic, and disorderly motions due to a coupling between the modes involved in the resonance. Highly low excitation levels were discovered to generate erratic motions under certain conditions.

An experimental analysis of the nonlinear behavior of an internally-resonant composite structural system to primary resonant excitation was presented by B. Balachandran and A. H. Nayfeh [3]. Nonlinear periodic, regularly modulated, and chaotically modulated responses arise from interaction between both the structure's directly and explicitly excited vibrational modes. Because of the relationship among flexural and tensional vibrational modes, too many of the described nonlinear responses are nonplanar. Weakly nonlinear analysis can be conducted to model the qualitative and quantitative reaction of an internal and external resonant structural configuration subjected to constrained primary resonant oscillations, as shown by B. Balachandran and A. H. Nayfeh [4]. The research can also be employed to forecast the Hopf bifurcation, defining the control component values at which regularly and chaotically modulated motions are most likely to appear. The effectiveness of a velocity feedback dependent nonlinear resonant controller to monitor the free and imposed self-excited vibration of a nonlinear beam was introduced by Joy Mondal and S. Chatterjee [5]. The nonlinear function of the derivative of the filter vector, which is transmitted via a second-order filter with the velocity stimulus from the sensor, is considered to evaluate the control power. Liang Li et al. [6] established a novel hierarchical methodology for turbulence analyses of rotating flexible beams with enhanced active restricted layer damping (EACLD) processing that is partly shielded for vibration surveys. Via simulating the EACLD patch's edge portion as an analogous spring with attached tip force the mass influence of the two inserted edge elements is utilized. The distinct rigid-flexible associated dynamic equations of hub-beam schemes with EACLD processing in open-loop and closed-loop circumstances was obtained through the asserted mode strategy and

Lagrange's equations. The beam is non-uniform and buckled at its left side to its disk's nucleus, where torque management operates, according to Boumediène and Smaoui [7], whereas a memory barrier control is located at the right end. The normal torque control is presented first, accompanied by the boundary control that is constructed using a particular form of memory phenomena as well as the dynamic characteristics of the input. Centered on a robust rotating beam vibration principle, an image recognition technique, and the lifting technique of data processing, L.F. Lyu and W.D. Zhu [8] introduced a new operational modal analysis (OMA) approach for a rotating structure. They created a tracking continually scanning laser Doppler vibrometer (TCSLDV) technique for controlling, scanning a rotating structure. Image processing was applied to specify the rotating structure's real-time situation allowing the TCSLDV device to detect a time-varying scanning path on the rotating structure.

To control the vibration of essentially assisted flexible plates, Sadek et al. [9] utilized piezoelectric-patch-actuators as active control. To measure actuator's voltage, an optimum control rule was inferred using the maximum principle theory. For directing polymer actuator displacement control, Wang et al. [10] adopted a reverse feed-forward controller system. The direct integration scheme [11] is used to analyze broad deformation study for a cantilever beam with a variable bending stiffness under both static and dynamic loads. Chentouf [12] investigated a model consisting of a nonhomogeneous flexible beam fastened to a rigid disc at its left end and free at its right end, where another rigid body is connected. They dealt with a variety of physical circumstances and devised feedback management rules to match. Kapuria and Yasin [13] investigated piezoelectric fiber-reinforced composite structures for successful vibration repression of metal laminated surfaces. Warminski et al. [14] investigated the experimental and theoretical motions of an autoparametric structure made up of two rectangular-sectioned beams. For irregular and harmonic oscillations, the experimental analysis of the system, configured at 1:4 internal resonance, is accomplished. Batista [15] derived the solution of large deflections of a beam within three-point bending in terms of Jacobi elliptical functions. Li et al. [16] and Peng et al. [17] implemented the effect of shear deformation and frictional end supports in the broad deformation of Timoshenko beam study. Huang et al. [18] recently used FIM to analyze static broad deformation under a dead focused vertical or horizontal force with exceptionally high precision. FIM is applied to the static/dynamic large deformation of a beam exposed to various types of loads using the Trapezoidal law and the integration matrix. Using the elliptic-function and the shooting process, Nguyen and Buntara [19] investigated broad deflections for uniform/non-uniform cantilever beams submitted to a moment at the top.

Zhang et al. [20] discussed the chaotic dynamics of a six-dimensional nonlinear structure that describes the averaged equation of a composite laminated piezoelectric rectangular plate subjected to transverse compression. The case of 1:2:4 internal resonances is considered, as well as in-plane excitations and

excitation filled by piezoelectric layers. Zhang and Li [21] investigated the resonant turbulent movements of a strictly assisted rectangular narrow plate with parametrically and externally excitations including exponential dichotomies and an averaging method. Sayed and Kamel [22, 23] reviewed the influence of various regulators on the vibrating mechanism, as well as the saturation control of a linear absorber, in order to minimize vibrations caused by rotor blade flapping motions. Both phase plane approaches and frequency response equations are used to analyze the numerical solution's stability. Kamel et al. [24] analyzed a configuration that was subjected to multiple excitation forces from the outside. The model is a two-degree-of-freedom device with a main system (machine head) and an absorber that simulates ultrasonic machining (USM). The perturbation method is used to extract the solution up to the second order approximation. Both phase-plane and frequency response functions are used to scrutinize the system's stability numerically. To minimize the vibrations of a hybrid Rayleigh–van der Pol–Duffing oscillator, the delayed velocity feedback control (DVFC) is used by Amer et al. [25]. This system is a one-degree-of freedom containing the cubic and fifth nonlinear terms and an external force. F. O. Darwesh et al. [26] investigated the effect of negative velocity feedback controller on a magnetic levitation system under External and parametric forces. They concluded that the control of linear velocity feedback is better to reduce the resulting vibration than the cubic one. Amer et al. [27] analyzed the vibration properties of a motor rotor and the effect of electro - mechanical couplers with multi-excitation forces and speed controller. They found that the velocity feedback controller is more effective for this system under the effect of external and parametric excitation forces in case of the worst resonance case. The dynamics of the dissipative system with a cubic nonlinear time-delayed of the type of the damping Duffing equation were investigated by Yusry O. El-Dib [28], they showed numerically that the time delay play dual roles in the stability behavior.

The aim of this research is to compare the effectiveness of delayed velocity feedback control (DVFC) strategies for significant vibrations of flexible composite beam structures to other previous studies that used different types of control systems. Approximate and numerical models are used to produce the results. The method of multiple scales perturbation technique is applied throughout to determine the approximation solution, whereas, the Rung-Kutta procedure of fourth order is applied for obtaining the numerical solution. The stability of the system is investigated applying both frequency response equations and phase-plane method. Also, the frequency and force-response curves are determined. The effects of all different parameters on system behavior are studied numerically. Comparisons between the numerical and analytical simulations are investigated.

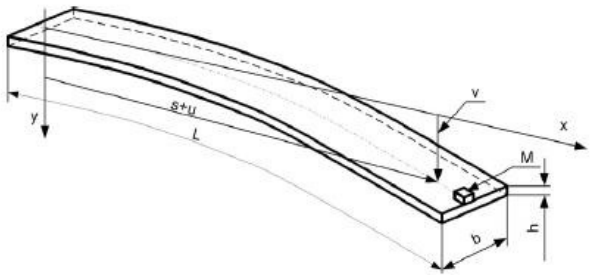

Figure 1: Semi-direct Shearer Drive Cutting Transmission Mechanism

2. System model and mathematical analysis

Consider the composite flexible beam in figure 1 given in [29] with a rectangular cross-section, the beam is assumed to be capable of significant flexural oscillations. The Hamilton's theory of last operation is used to derive the equation of motion for the current beam model. The same procedure, but for more complicated beam system, is shown in Warminske et al. [30]. The model is considered as the Euler- Bernoulli beam with added nonlinear curvature component $\rho_\nu = \nu''[1 + \frac{1}{2}(\nu')^2]$.
The dimensionless equation of motion takes form:

$$\nu + \nu^{IV}(1 + \nu'^2) + 4\nu'''\nu''\nu'^3 = \lambda\nu'', \tag{1}$$

where $\lambda = -\frac{1}{2}\int_1^s \int_0^s \nu'^2\, ds\, ds.$ is the Lagrange multiplier.

The horizontal and vertical displacements of the first vibration mode are taken into consideration in further investigations using Galerkin's approach [31] on system (1). The linear cantilever beam is supposed to be near to the function of the mode shape [29]. In the Galerkin's orthogonalization technique, the mode of the corresponding linear system is utilized As a result, we have a nonlinear ordinary differential equation for the first bending mode (based on a linear mode shape in the orthogonalization procedure):

$$\ddot{X} + 2\mu\,\omega\,\dot{X} + \omega^2 X + \beta X^3 - \delta(X\,\dot{X}^2 + X^2\ddot{X}) = 0, \tag{2}$$

where X is the generalized coordinate that corresponds to the displacement of the beam's tip, are the damping, cubic nonlinear term coefficients. The analysis is performed for an epoxy, carbon fiber reinforced beam with physical parameters [29]: $\rho = 2100\frac{kg}{m^3}$, $b = 12.8mm$, $h = 1mm$, $l = 236mm$, $M = 5 * 10^{-4}kg$, and the dimensionless coefficients $\omega^2 = 9.382, \beta = 14.4108, \delta = 0.930024, \mu = 0.01$. The oscillations of the nonlinear composite beam model are described by adapted nonlinear differential equations (with various types of controllers) in

[32, 33, 34, 35]. In this paper, the system with delayed velocity feedback control (DVFC) is given by:

$$\begin{aligned} &\ddot{p} + 2\varepsilon\ \hat{\mu}\ \omega\ \dot{p} + \omega^2 p\varepsilon\ \hat{\alpha} p^3 - \varepsilon\ \hat{\delta}(\, p\ \dot{p}^2 + p^2 \ddot{p}) \\ &= \varepsilon(\ \hat{f}_1 \cos(\Omega_1 t) + \ p\, \hat{f}_2 \cos(\Omega_2 t) - \ \hat{G}\ \dot{p}(\, t - \tau)), \end{aligned} \tag{3}$$

where $\hat{\mu} = \frac{\mu}{\varepsilon}, \hat{\alpha} = \frac{\alpha}{\varepsilon}, \hat{\delta} = \frac{\delta}{\varepsilon}, \hat{f}_1 = \frac{f_1}{\varepsilon},\ \hat{f}_2 = \frac{f_2}{\varepsilon},\ \hat{G} = \frac{G}{\varepsilon}, p$ represent the composite beam system displacement, μ is the viscous damping coefficient, ω is the natural frequency accompanied by the composite beam, $f_n, \Omega_n, n = 1, 2$ are the excitation forces and the excitation frequencies, and α, δ are the main system nonlinear stiffness coefficient which may be due to material of the beam nonhomogeneity.

2.1 Perturbation analysis

The second order approximation is given by applying the Multiple Time Scales (MTSM) procedure [36] so $p(t)$ in power series form will be:

$$p(\, T_o,\, T_1, \varepsilon) = \ p_o(\, T_o,\, T_1) + \varepsilon\, p_1(\, T_o,\, T_1) + \ O(\varepsilon^2), \tag{4}$$

where the time derivative takes the values:

$$\frac{d}{dt} = D_0 + \varepsilon D_1 + O(\varepsilon^2),\ \frac{d^2}{dt^2} = D_o^2 + 2\varepsilon D_0 D_1 + O(\varepsilon^2) \tag{5}$$

and $T_n = \varepsilon^n t,\ \ D_n = \frac{\partial}{\partial T_n},\ n = 0, 1.$

Switching equations (4), (5) into (3) and equating same power of ε coefficients to take out:

$$\begin{aligned} &O(\varepsilon^0): \\ &\qquad (D_o^2 + \omega^2)\, p_0 = 0, \end{aligned} \tag{6}$$

$$\begin{aligned} &O(\varepsilon): \\ &(D_o^2 + \omega^2)\, p_1 = -2\, D_o\, D_1\, p_o - \ 2\hat{m}u\omega\, D_o\, p_o\ + \hat{f}_1 \cos(\Omega_1\, t) \\ &+ \hat{f}_2\, p_o \cos(\Omega_2\, t) - \hat{\alpha}\, p_o^3\ + \hat{\delta}\, p_0[(\, D_o\, p_o)^2 + \ p_o(\, D_o^2\, p_o)] - \ G\, D_o\, p_{o\tau}. \end{aligned} \tag{7}$$

And the homogeneous solution of (6)is given by:

$$p_0 = A(T_1)\, e^{i\omega\, T_0} + \ cc, \tag{8}$$

where cc represents the complex conjugate of the preceding term, and A is complex function in T_1.

Let:

$$\begin{aligned} p(t - \tau) &= \ p_{o\tau}(T_o, T_1) + \varepsilon\, p_{1\tau}(T_o, T_1) + \ O(\varepsilon^2) \\ &= \ p_o(\, t - \tau, \varepsilon(\, t - \tau)) + \varepsilon\, p_1(\, t - \tau, \varepsilon(\, t - \tau)) + \ O(\varepsilon^2), \end{aligned} \tag{9}$$

where

$$
\begin{aligned}
& p_o(t-\tau, \varepsilon(t-\tau)) = p_{o\tau}(t, \varepsilon t) = p_{o\tau}(T_o, \varepsilon T_1), \\
& p_1(t-\tau, \varepsilon(t-\tau)) = p_{1\tau}(t, \varepsilon t) = p_{1\tau}(T_o, \varepsilon T_1).
\end{aligned} \tag{10}
$$

using equation (8), yields:

$$
\begin{aligned}
& p_{o\tau}(t, \varepsilon t) = p_o(t-\tau, \varepsilon(t-\tau)) \\
& = A(\varepsilon(t-\tau))\, e^{i\omega(t-\tau)} + \bar{A}(\varepsilon(t-\tau))\, e^{-i\omega(t-\tau)} \\
& = A(T_1 - \varepsilon\tau) e^{i\omega(t-\tau)} + \bar{A}(T_1 - \varepsilon\tau)\, e^{-i\omega(t-\tau)}.
\end{aligned} \tag{11}
$$

now expanding $A(T_1) - \varepsilon\tau)$ using Taylor series:

$$
A(T_1 - \varepsilon\tau) = A(T_1) - \varepsilon\tau \dot{A}(T_1) + \cdots \simeq A(T_1) + O(\varepsilon^2). \tag{12}
$$

Substituting (12) into **??** and using only the first term approximation so:

$$
p_{o\tau}(T_o, T_1) = A(T_1) e^{i\omega(To-\tau)} + \bar{A}(T_1) e^{-i\omega(To-\tau)}. \tag{13}
$$

Introducing (8), and (13) into 7, yields:

$$
\begin{aligned}
(D_o^2 + \omega^2) p_1 = & -2(i\omega D_1 A e^{i\omega T_o} - i\omega D_1 \bar{A} e^{-i\omega T_o}) \\
& - 2\omega\hat{\mu}(i\omega A e^{i\omega T_o} - i\omega \bar{A} e^{-i\omega T_o}) - \hat{\alpha}((A e^{i\omega T_o} - \bar{A} e^{-i\omega T_o})^3) \\
& + \hat{\delta}(A e^{i\omega T_o} - \bar{A} e^{-i\omega T_o})((i\omega A e^{i\omega T_o} - i\omega \bar{A} e^{-i\omega T_o})^2) \\
& - (\omega^2)\hat{\delta}((A e^{i\omega T_o} - \bar{A} e^{-i\omega T_o})^2) + \frac{\hat{f}_1}{2}(e^{i\Omega_1 T_o} - e^{-i\Omega_1 T_o}) \\
& + \frac{\hat{f}_2}{2}(A e^{i\omega T_o} - \bar{A} e^{-i\omega T_o})(e^{i\Omega_2 T_o} - e^{-i\Omega_2 T_o}) \\
& - G(i\omega A e^{i\omega(T_o-\tau)} - i\omega \bar{A} e^{-i\omega(T_o-\tau)}).
\end{aligned} \tag{14}
$$

We study now the system's severe operating approaches due to the resonance case, the worst case is the combined primary and subharmonic case i.e.:

$$
\Omega_1 = \omega + \varepsilon\,\sigma_1, \Omega_2 = 2\,\omega + \varepsilon\,\sigma_2, \tag{15}
$$

where $\sigma_i, i = 1, 2$ are called the detuning parameters. Inserting (15) into (14) and eliminating coefficients of all secular terms, yields:

$$
-2i\omega D_1 A - 2i\hat{\mu}\omega^2 A - 3\hat{\alpha}A^2\bar{A} + \frac{\hat{f}_1}{2} e^{i\sigma_1 T_1} + \frac{\hat{f}_2 \bar{A}}{2} e^{i\sigma_2 T_1} - Gi\omega A e^{i\omega\tau} = 0. \tag{16}
$$

Converting A into the polar form:

$$
A = \frac{a}{2} e^{i\gamma},\ D_1 A = \frac{e^{i\gamma}}{2}[\dot{a} + i\, a\, \dot{\gamma}], \tag{17}
$$

where a and γ are the system amplitude and phase, respectively.
Introducing (17) into (16) and comparing the real and imaginary parts in the resulting equation, then we get:

$$\dot{a} = -\mu\omega\, a + \frac{\hat{f}_1 \sin(\theta_1)}{2\omega} + \frac{\hat{f}_2 \sin(\theta_2)}{4\omega} - \frac{G\, a\, \cos(\omega\tau)}{2}, \tag{18}$$

$$a\,\dot{\theta_1} = \sigma_1\, a - \frac{3\,\hat{\alpha}\, a^3}{8\,\omega} - \frac{\omega\hat{\delta}\, a^3}{4} + \frac{\hat{f}_1 \cos(\theta_1)}{2\,\omega} + \frac{\hat{f}_2\, a\, \cos(\theta_2)}{4\,\omega} - \frac{G\, a\, \sin(\omega\tau)}{2}, \tag{19}$$

where

$$\theta_1 = \sigma_1 T_1 - \gamma, \quad \theta_2 = \sigma_2 T_1 - 2\,\gamma. \tag{20}$$

2.2 Steady state solution

The amplitude and phase steady state solution is obtained by substituting $\dot{a} = \dot{\theta_1} = 0$ into Eqs. (18), and (19), then we obtain:

$$\frac{\hat{f}_1 \sin(\theta_1)}{2\,\omega} + \frac{\hat{f}_2\, a\, \sin(\theta_2)}{4\,\omega} = \hat{mu}\omega\, a + \frac{G\, a\, \sin(\omega\tau)}{2}, \tag{21}$$

$$\frac{\hat{f}_1 \cos(\theta_1)}{2\,\omega} + \frac{\hat{f}_2\, a\, \cos(\theta_2)}{4\,\omega} = \frac{3\hat{\alpha}\, a^3}{8\omega} + \frac{\omega\hat{\delta}\, a^3}{4} + \frac{G\, a\, \sin(\omega\tau)}{2} - \sigma_1\, a\,. \tag{22}$$

Squaring and adding equations (21) and (22) to have the frequency response equation in the form:

$$\Gamma_1\, a^6 + \Gamma_2\, a^5 + \Gamma_3\, a^4 + \Gamma_4\, a^3 + \Gamma_5\, a^2 + \Gamma_6\, a + \Gamma_7 = 0, \tag{23}$$

where:

$$\begin{aligned} &\Gamma_1 = (\frac{3\,\hat{\alpha}}{8\,\omega} + \frac{\omega\hat{\delta}}{4})^2, \Gamma_2 = 0, \Gamma_3 = (\frac{G\, \sin(\omega\tau)}{2} - \sigma_1)(\frac{3\,\hat{\alpha}}{4\,\omega} + \frac{\omega\hat{\delta}}{2}), \\ &\Gamma_4 = 0, \Gamma_5 = (\hat{\mu}\omega + \frac{G\sin(\omega\tau)}{2})^2 + (\frac{G\sin(\omega\tau)}{2} - \sigma_1)^2 - \frac{\hat{f_2}^2}{16\,\omega^2}, \\ &\Gamma_6 = -\frac{\hat{f}_1\hat{f}_2}{4\omega^2}, \Gamma_7 = -\frac{\hat{f_1}^2}{4\omega^2}, \sigma_2 = 2\,\sigma_1. \end{aligned} \tag{24}$$

2.3 Stability analysis

Linearizing equations (18), and (19) according to the Lyapunov first (indirect) form [37, 38, 39] to address the stability behavior of these solutions, to give the following system:

$$\begin{bmatrix} \dot{a} \\ \dot{\theta}_1 \end{bmatrix} = J \begin{bmatrix} a \\ \theta_1 \end{bmatrix} = \begin{bmatrix} \upsilon_{11} & \upsilon_{12} \\ \upsilon_{21} & \upsilon_{22} \end{bmatrix} \begin{bmatrix} a \\ \theta_1 \end{bmatrix}, \tag{25}$$

where

$$
\begin{aligned}
\upsilon_{11} &= \frac{\partial \dot{a}}{\partial a} = -\hat{\mu}\omega + \frac{\hat{f}_2 \sin(2\,\theta_1)}{4\,\omega} - \frac{G\,\sin(\omega\tau)}{2},\\
\upsilon_{12} &= \frac{\partial \dot{a}}{\partial \theta_1} = \frac{\hat{f}_1 \cos(\theta_1)}{2\,\omega} + \frac{\hat{f}_2\, a\, \cos(2\,\theta_1)}{2\,\omega},\\
\upsilon_{21} &= \frac{\partial \dot{\theta_1}}{\partial\, a} = \frac{\sigma_1}{a} - \frac{9\hat{\alpha}\, a}{8\omega} - \frac{3\omega\hat{\delta}\, a}{4} + \frac{\hat{f}_2 \cos(2\,\theta_1)}{4\,\omega\, a} - \frac{G\,\sin(\omega\tau)}{2\,\omega},\\
\upsilon_{22} &= \frac{\partial \dot{\theta_1}}{\partial \dot{\theta_1}} = -\frac{\hat{f}_1 \sin(\theta_1)}{2\,\omega\, a} - \frac{\hat{f}_2 \sin(2\,\theta_1)}{2\,\omega}.
\end{aligned}
\tag{26}
$$

The stability of the steady-state solution therefore, depends on the Jacobian matrix's eigenvalues that can be obtained by solving the following characteristic equation:

$$
\begin{vmatrix} \upsilon_{11} - \lambda & \upsilon_{12} \\ \upsilon_{21} & \upsilon_{22} - \lambda \end{vmatrix} = 0, \tag{27}
$$

or

$$
\lambda^2 - tr(J)\lambda + \left| J \right| = 0, \tag{28}
$$

where λ denotes the Jacobian matrix $\left| J \right|$ eigenvalues, As shown by the Routh-Huriwitz criterion [40] the solution of the state is asymptotically stable if and only if

$$
tr(J) > 0, \left| J \right| > 0. \tag{29}
$$

Routh-Huriwitz conditions (29) are established numerically with the help of MATLAB software for estimating the stable and the unstable regions in the frequency response curves.

3. Results and discussion

In this section, the behavior of the system's amplitude and phase in resonance and non-resonance situations are demonstrated. The Rung-Kutta procedure of order four is utilized to evaluate the numerical solution of the given scheme, supposing the following parameters: $\mu = 0.001, f_1 = 0.01, f_2 = 0.05, \delta = 0.0001, \alpha = 0.002, \omega = 4$.

The time response is seen in Figure 1 (a) magnitudes at non-resonant situation and without control ($\Gamma = 0$), where Figure 2 (b) represents the system phase plane, the periodic solution is shown with asymptotically stable situation. Figure 3 (a) shows the time response for the system without applying control with resonance instance, $\Omega_1 = \omega + \varepsilon\,\sigma_1$, $\Omega_2 = 2\,\omega + \varepsilon\sigma_2$, furthermore, a Poincaré maps obtained in Figure 3 (b) for uncontrolled system at the same parameters. We observe that trajectory approaches a center of the graph in a very long

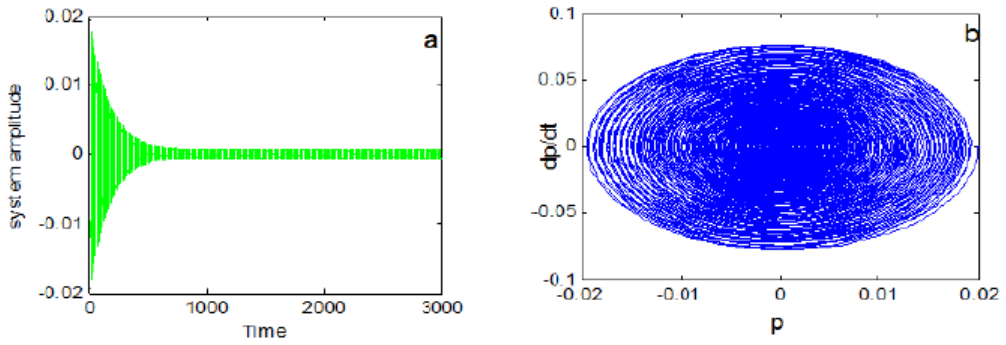

Figure 2: Time response in the normal operation (without resonance) and without applying control. (b) System phase plane.

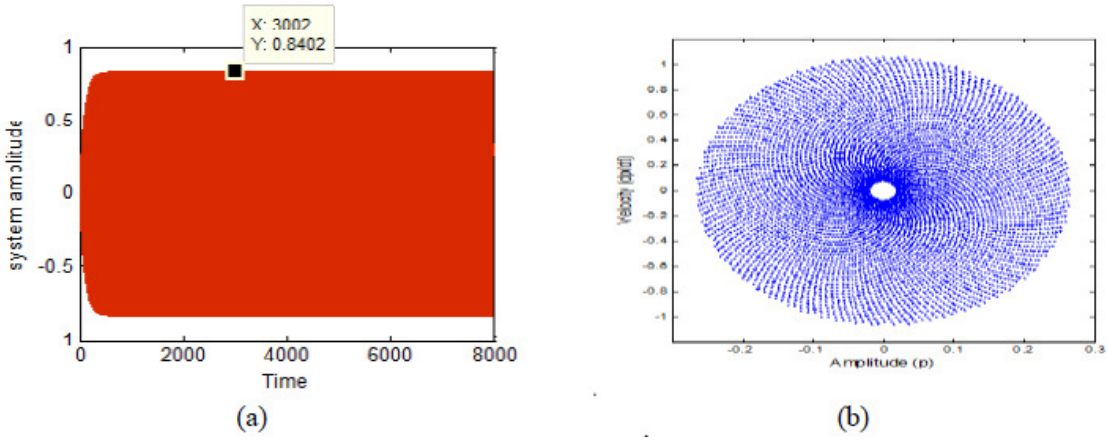

Figure 3: (a) Time response in the resonance case $\Omega_1 = \omega$, $\Omega_2 = 2\,\omega$ and without applying control ($G = 0$). (b) Poincaré mapping without control ($G = 0$).

time (stable center). The influence of applying delayed velocity feedback control (DVFC) on the system is clarified in Figure 4 (a),$G = 1.5$, $\tau = 0.274$, while Figure 4 (b) shows Poincaré maps obtained for the controlled model and trajectory approaches a center of the graph in a very short time compared to uncontrolled model. Figure 5 shows a comparison between the (DVFC) and active control introduced in [32]. From this figure, we conclude that the (DVFC) is more effective than the previous work in [32] and also more effective than the delayed control in the displacement. The effective of (DVFC) is about 99.93%where the active control introduced in [32] it is about 96.71 %. Another one important advantage of using (DVFC) is that the system reaches the steady state more

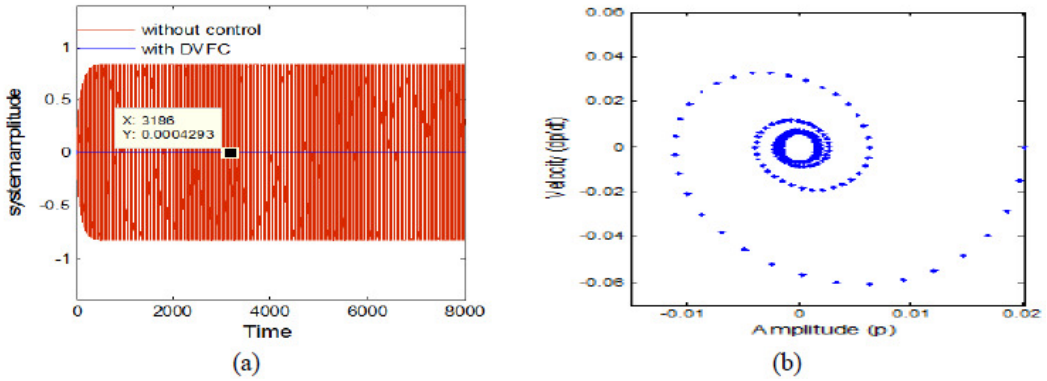

Figure 4: (a) Time response in the resonance case and with applying DVFC,($G = 1.5$) (blue curve) and without applying control ($G = 0$) (red curve). (b) Poincaré mapping with control ($G = 1.5$, $\tau = 0.274$).

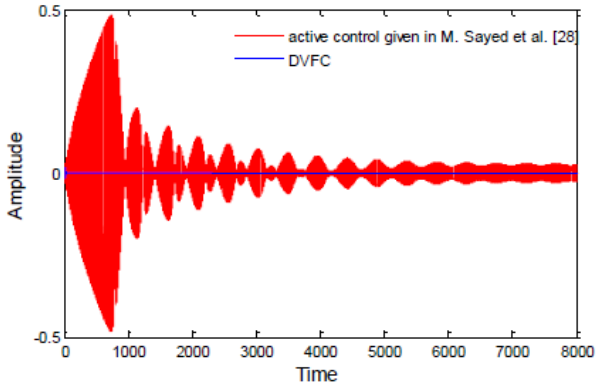

Figure 5: Comparison between (DVFC) and active control given in [32], $G = 1.5$, for both case.

rapidly than the case of active control introduced in M. Sayed et al. [32]. In Figure 6, for controlled processes with $G = 1.5$, $\tau = 0.274$, and near resonance case $\Omega_1 = \omega + \varepsilon\,\sigma_1$, $\Omega_2 = 2\,\omega + \varepsilon\,\sigma_2$, the response curve is shown for different values of the external force $f_1 = 0.01,\ 0.05,\ 0.1$. This curves show that, system peaks is proportional to f_1, and inversely proportional to the damping coefficient μ as shown in Figure 7 for. Figure 8 illustrate the frequency response by applying different values for the controller gain G, the figure clarify the inverse relation between the amplitude and the gain . Modifying the original natural frequency ω of the system modes changes the amplitudes in the response curves inversely, as clarified in Figures 9 at the values $\omega = 0.5, 1, 2$. Both solution

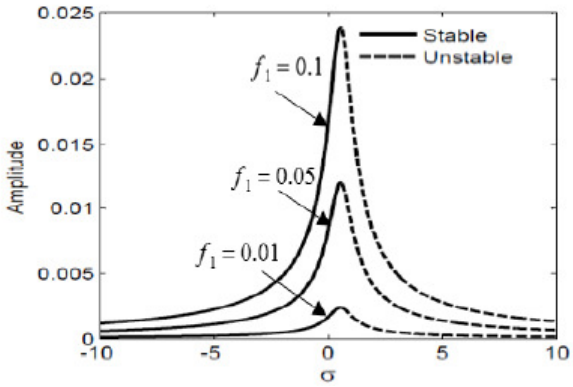

Figure 6: Effect of external excitation f_1, $f_1 = 0.01, 0.05, 0.1$, $G = 1.5$, $\tau = 0.274$).

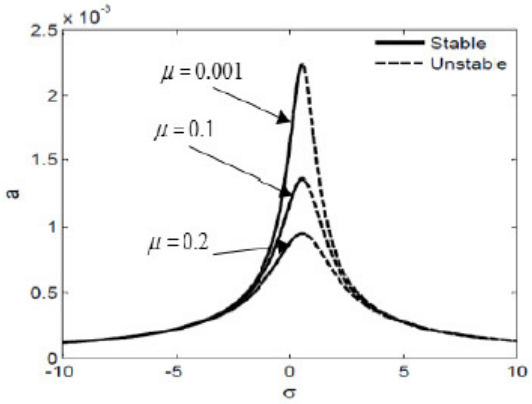

Figure 7: Effect of damping coefficient $\mu, \mu = 0.01, 0.1, 0.2$, $G = 1.5$, $\tau = 0.274$).

induced by (MTSM) and numerical solution using Rung-Kutta Method (RKM) of fourth order are matched in Figures 10-13 for time history and frequency response curves for the system. Figure 10, show good agreement between the approximate solution (blue curve) and the numerical outcome (green curve) of the resonance case without applying control scheme, while time response with applying (DVFC) is shown in Figures 11 by applying both RKM and MTSM at $G = 1.5$. Good results for the frequency response between the numerical and approximate method for frequency response at $G = 1.5, G = 0$ are shown in Figures 12, and 13 respectively. The change of amplitude range with varying of the delay time τ is shown in Figure 14, we observe that the optimum range for the time delay on the velocity feedback controller is $0 \leq \tau < 0.347$. Parameters effect on the system amplitude are illustrated on Figures 15, 16, the system

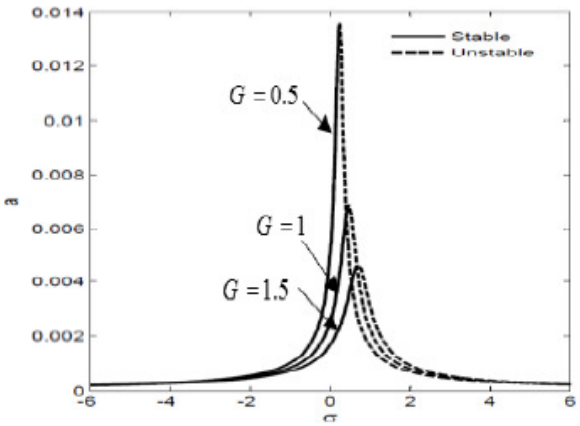

Figure 8: Effect of controller gain G, $G = 0.5, 1, 1.5$, $\tau = 0.274$).

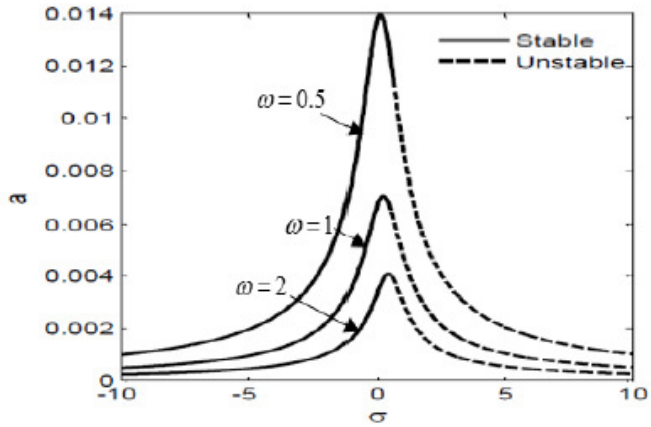

Figure 9: Effect of natural frequency $\omega, \omega = 0.5, 1, 2$, $G = 1.5$, $\tau = 0.274$).

mounts is decreased with the increase of the damping coefficient μ, we observed that from Figure 15, the optimum damping coefficient is $\mu > 0.1$, the system will has minimum amplitude and will be asymptotically stable with larger values of μ, but we cannot find a material with suitable value of damping coefficient or it can be found with highly costs, so we use a suitable material for the system and adding controller like (DVFC) for saving the system from damaging during resonance states and save system stability. A suitable value for controller gain $G > 0.5$ is illustrated in Figure 16.

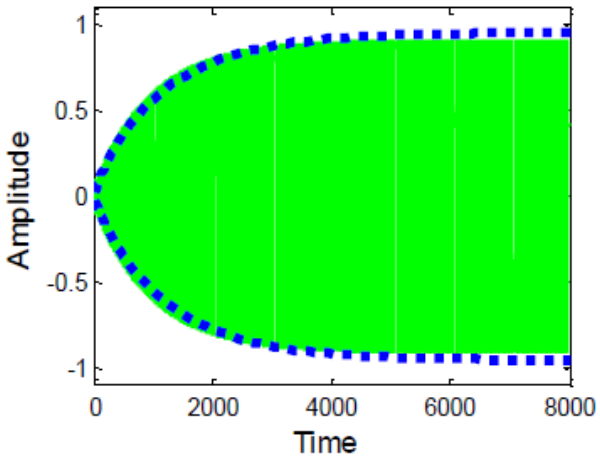

Figure 10: Comparison between numerical results (green curve) and approximate solution (blue curve), $G = 0$.

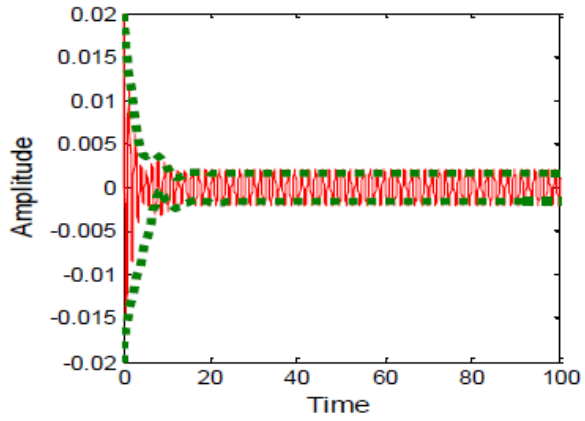

Figure 11: Comparison between numerical results (red curve) and approximate solution (green curve), $G = 1.5$, $\tau = 0.274$).

4. Conclusion

A dynamical representation of structural model architecture exhibiting a nonlinear composite cantilever beam with multi-excitation forces was investigated and solved in this analysis using multiple time scales methodology. The tragic resonance events were treated using the delayed velocity feedback control DVFC. The effective range for the delay time on the velocity feedback controller have been given by $0 \leq \tau < 0.34$. The worse situation of resonance is the simultaneous case ($\Omega_1 = \omega$, $\Omega_2 = 2\omega$). The amplitude of the composite beam was

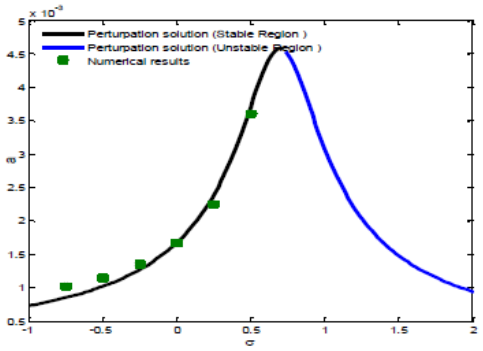

Figure 12: Comparison between numerical results and approximate solution with resonance, $G = 1.5$, $\tau = 0.274$).

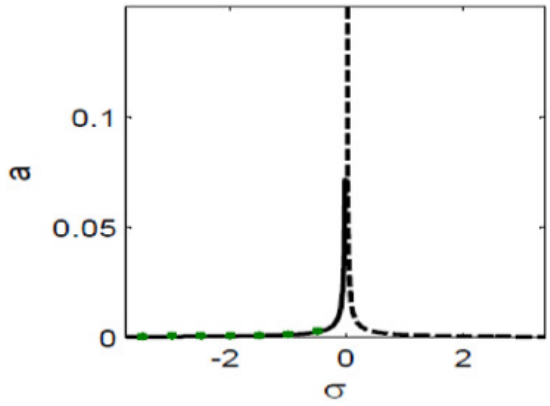

Figure 13: Comparison between numerical results (green curve) and approximate stable solution (solid black curve), with resonance, $G = 0$.

increased to about 1203 times of the excitation forces amplitude at resonance instance. The impact of DVFC was explained and debated. The control effect was found to be 99.93 ٪according to the DVFC result, and 96.71 ٪due to the effect of the active control applied in the previous work for M. Sayed et al. [32], implying that the DVFC was more efficient for this device in the resonance situation. An appropriate stability analysis was also performed and adequate feedback gains are detected in order to significantly reduce the amplitude peak and increase the stability region. Furthermore, numerical formulations achieved through using fourth-order Rung-Kutta technique were compared to approximate solutions derived via the multiple scales method. Both approximately and numerical techniques, the comparison provided strong consensus. Finally, the

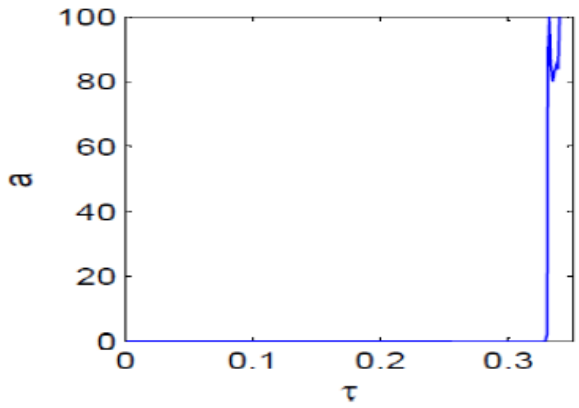

Figure 14: Effect of the time delay on the amplitude.

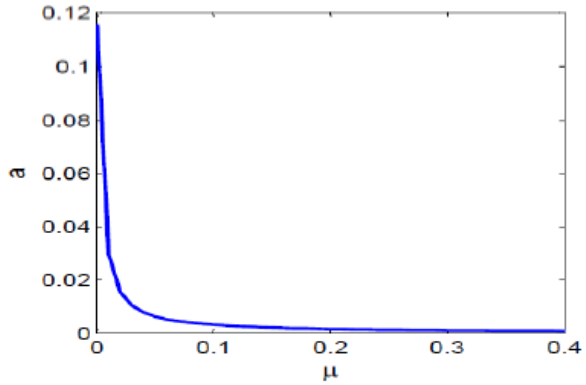

Figure 15: Effect of the damping coefficient on the amplitude.

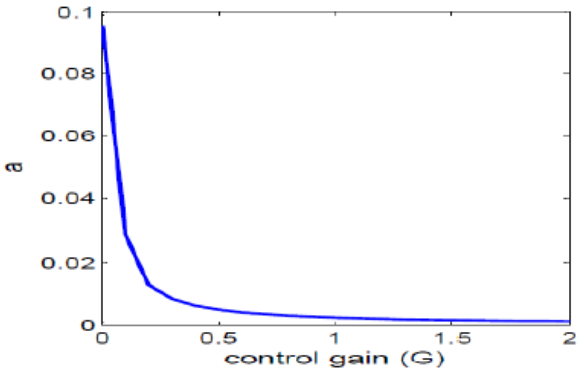

Figure 16: Effect of the controller gain on the amplitude.

influence of parameters on the scheme amplitude and the implications for the system's stability requirements were planned.

Acknowledgement

The authors would like to thank the anonymous referee for the constructive comments that improved the paper.

References

[1] A. H. Nayfeh, B. Balachandran, *Modal interactions in dynamical and structural systems,* Applied Mechanics Reviews, 42 (1989), 175-202.

[2] A. H. Nayfeh, B. Balachandran, M. A. Colbert, M. A. Nayfeh, *An experimental investigation of complicated responses of a two-degree-of-freedom structure,* ASME Journal of Applied Mechanics, 56 (1989), 960-967.

[3] B. Balachandran, A. H. Nayfeh, *Nonlinear oscillations of a harmonically excited composite structure,* Composite Structures, 16 (1990), 323-339.

[4] B. Balachandran, A. H. Nayfeh, *Nonlinear motions of beam-mass structure,* Nonlinear Dynamics, 1 (1990), 39-61.

[5] Joy Mondal, S. Chatterjee, *Controlling self-excited vibration of a nonlinear beam by nonlinear resonant velocity feedback with time-delay,* International Journal of Non-Linear Mechanics, 131 (2021), 103684.

[6] Liang Li, Wei-Hsin Liao, Dingguo Zhang, Yongbin Guo, *Dynamic modeling and analysis of rotating beams with partially covered enhanced active constrained layer damping treatment,* Journal of Sound and Vibration, 455 (2019), 46-68

[7] Boumediène Chentouf, Nejib Smaoui, *Exponential stabilization of a non-uniform rotating disk-beam system via a torque control and a finite memory type dynamic boundary control,* Journal of the Franklin Institute, 356 (2019), 11318–11344.

[8] L.F. Lyu, W.D. Zhu, *Operational modal analysis of a rotating structure under ambient excitation using a tracking continuously scanning laser Doppler vibrometer system,* Mechanical Systems and Signal Processing, 152 (2021), 107367.

[9] Sadek I.S., Kucuk I., Adali S., *Active open-loop control of plates with multiple piezoelectric patches via the maximum principle,* Mech. Adv. Materials Structures, 21 (2014), 772–779.

[10] Wang X., Alici G., Tan X., *Modeling and inverse feedforward control for conducting polymer actuators with hysteresis,* Smart Materials Structures, 23 (2014), 25015–25023.

[11] Wei, H., Pan, Q.X., Adetoro, O.B., Avital, E., Yuan, Y., Wen, P.H., *Dynamic large deformation analysis of a cantilever beam,* Math. Comput. Simulation, 174 (2020), 183–204.

[12] Chentouf, B., *Modelling and stabilization of a nonlinear hybrid system of elasticity,* App. Math. Model, 39 (2015), 621–629.

[13] Kapuria, S., Yasin, M.Y., *Active vibration suppression of multilayered plates integrated with piezoelectric fiber reinforced composites using an efficient finite element model,* J. Sound Vib., 329 (2010), 3247–3265.

[14] Warminski, J., Cartmell, M.P., Bochenski, M., Ivanov, I., *Analytical and experimental investigations of an autoparametric beam structure,* J. Sound Vib., 315 (2008), 486–508.

[15]] M. Batista, *Large deflections of a beam subjected to three-point bending,* Int. J. Non-Linear Mech., 69 (2015), 84–92.

[16] X.-F. Li, H. Zhang, K.Y. Lee, *Dependence of Young's modulus of nanowires on surface effect,* Int. J. Mech. Sci., 81 (2014), 120–125.

[17] X.-L. Peng, X.-F. Li, G.-J. Tang, Z.-B. Shen, *Effect of scale parameter on the deflection of a nonlocal beam and application to energy release rate of a crack Z,* Angew. Math. Mech, 95 (2015), 1428–1438.

[18] T. Huang, Y. Yuan, J.L. Zheng, E. Avital, P.H. Wen, *Large deformations of tapered beam with finite integration method,* Eng. Anal. Bound Elem, 82 (2017), 32–42.

[19] D.K. Nguyen, S.G. Buntara, *Large deflections of tapered functionally graded beams subjected to end forces,* Applied Mathematical Modelling, 38 (2014), 3054-3066.

[20] W. Zhang, M. Gao, M. Yao, Z. Yao, *Higher dimensional chaotic dynamics of a composite laminated piezoelectric rectangular plate,* Science in China Series Physics Mechanics and Astronomy, 52 (2009), 1989-2000.

[21] W. Zhang, S. B. Li, *Resonant chaotic motions of a buckled rectangular thin plate with parametrically and externally excitations,* Nonlinear Dynamics, 62 (2010), 673-686.

[22] M. Sayed, M. Kamel, *1:2 and 1:3 internal resonance active absorber for non-linear vibrating system,* Applied Mathematical Modelling, 36 (2012), 310-332.

[23] M. M. Kamel, W. A. EL-Ganaini, Y. S. Hamed, *Vibration suppression in ultrasonic machining described by nonlinear differential equations via passive controller,* Applied Mathematics and Computation, 219 (2013), 4692-4701.

[24] A. H. Nayfeh, *Perturbation methods,* New York, Wiley, Chap., 6 (1973), 228-243.

[25] Amer Y. A., El-Sayed A. T., Abd El-Salam M. N.,, *Position and velocity time delay for and suppression vibrations of a hybrid Rayleigh-Van der Pol-Duffing oscillator,* Journal of sound & vibration, 54 (2020), 149-161.

[26] F. O. Darwesh, Y. A. Amer, K. R. Raslan, *Effect of the negative velocity feedback control for reducing the primary resonance vibration of a magnetic levitation system using the harmonic balance method,* Appl. Math. Inf. Sci., 15 (2021), 365-372.

[27] Y. A. Amer, Taher A. Bahnasy, Ashraf M. Elmhlawy, *Vibration analysis of permanent magnet motor rotor system in shearer semi-direct drive cutting unite with speed controller and multi- excitation forces,* Appl. Math. Inf. Sci., 15 (2021), 373-381.

[28] Yusry O. El-dib, *Periodic solution and stability behavior for nonlinear oscillator having a cubic nonlinearity time-delayed,* International Annals of Science, 5 (2018), 12-25.

[29] Jerzy Warminski, Marcin Bochenski, Wojciech Jarzyna, Piotr Filipek, Michal Augustyniak, *Active suppression of nonlinear composite beam vibrations by selected control algorithms,* Com. Nonlinear Sci. Num. Sim., 16 (2011), 2237–2248.

[30]] J. Warminski, M. P. Cartmell, M. Bochenski, I. Ivanov, *Analytical and experimental investigations of an autoparametric beam structure,* Journal of Sound Vibration, 315 (2008), 486-508.

[31] Andrea Bonito, Ricardo H. Nochetto, Dimitris Ntogkas, *Discontinuous Galerkin approach to large bending deformation of a bilayer plate with isometry constraint,* Journal of Computational Physics, 423 (2020), 109785,

[32]] M. Sayed, A. A. Mousa, D. Y. Alzaharani, I. H. Mustafa, S. I. El-Bendary, *Bifurcation analysis of a composite cantilever beam via 1:3 internal resonance,* Journal of the Egyptian Mathematical Society, 2020.

[33] Warminski, J., Cartmell, M.P., Bochenski, M., Ivanov, I., *Analytical and experimental investigations of an autoparametric beam structure,* J. Sound Vib., 315 (2008), 486–508.

[34] Warminski, J., Bochenski, M., Jarzyna, W., Filipek, P., Augustyniak, M., *Active suppression of nonlinear composite beam vibrations by selected control algorithms,* Commun. Nonlinear Sci Numerical Simulation, 16 (2011), 2237–2248.

[35] Hamed, Y.S., Amer, Y.A., *Nonlinear saturation controller for vibration supersession of a nonlinear composite beam,* J. Mech. Sci. Technol, 28 (2014), 2987–3002.

[36] Nayfeh, A.H., Mook, D.T., *Nonlinear oscillations,* Wiley, New York, 1995.

[37] Slotine, J.-J.E., Li, W., *Applied nonlinear control,* Prentice Hall, Englewood Cliffs, 1991.

[38] M. R. M. Rao, *Ordinary differential equations, theory and applications,* Edward Arnold, London, 1981.

[39] Bo Zhang, *Stability and Liapunove functions for fractional differential equations,* Math. Comput. Sci. Working, 2012.

[40] E. Ahmed, A.M.A. El-sayed, Hala A.A. El-saka, *On some Routh-Hurwitz conditions for fractional order differential equations and their applications in Lorenz,*, Rossler, Chua chen systems. Physics Letters A, 358 (2006), 1-4.

Accepted: May 15, 2021